ORNL/TM-2020/1451
Revision 0

Safety Testing and Destructive Examination of AGR-2 UO_2 Compact 3-1-1

John D. Hunn
Robert N. Morris
Fred C. Montgomery
Darren J. Skitt
Zachary M. Burns

February 2020

OAK RIDGE NATIONAL LABORATORY
MANAGED BY UT-BATTELLE FOR THE US DEPARTMENT OF ENERGY

ORNL/TM-2019/1451

Reactor and Nuclear Systems Division

SAFETY TESTING AND DESTRUCTIVE EXAMINATION OF AGR-2 UO_2 COMPACT 3-1-1

John D. Hunn
Robert N. Morris
Fred C. Montgomery
Darren J. Skitt
Zachary M. Burns

Revision 0

Date Published: February 2020

Work sponsored by
US DEPARTMENT OF ENERGY
Office of Nuclear Energy—Advanced Reactor Technologies
under the
Advanced Gas Reactor Fuel Development and Qualification Program

Prepared by
OAK RIDGE NATIONAL LABORATORY
Oak Ridge, TN 37831-6283
managed by
UT-BATTELLE, LLC
for the
US DEPARTMENT OF ENERGY
under contract DE-AC05-00OR22725

CONTENTS

REVISION LOG

Revision	Date	Affected pages	Revision description
0		All	Initial issue

LIST OF FIGURES

LIST OF TABLES

ABBREVIATIONS

AGR	Advanced Gas Reactor (Fuel Development and Qualification Program)
AGR-2	second AGR program irradiation experiment
AGR-5/6/7	fifth, sixth, and seventh AGR program irradiation experiments
CCCTF	Core Conduction Cooldown Test Facility
CO	carbon monoxide
DLBL	deconsolidation leach-burn-leach
FIMA	fissions per initial metal atom
ID	identification
IMGA	Irradiated Microsphere Gamma Analyzer
OPyC	outer pyrolytic carbon (TRISO layer)
ORNL	Oak Ridge National Laboratory
SiC	silicon carbide (TRISO layer)
TA_{max}	time-average maximum temperature
TA_{min}	time-average minimum temperature
TAVA	time-average, volume-average temperature
TRISO	tristructural isotropic (coated particles)
UCO	uranium carbide and uranium oxide (fuel kernels)
UO_2	uranium oxide (fuel kernels)

ACKNOWLEDGMENTS

This work was sponsored by the US Department of Energy Office of Nuclear Energy Advanced Reactor Technologies as part of the Advanced Gas Reactor Fuel Development and Qualification Program. Analysis of leach solutions and Core Conduction Cooldown Test Facility furnace components was conducted by the Oak Ridge National Laboratory (ORNL) Nuclear Analytical Chemistry and Isotopics Laboratory. Hot cell activities were supported by ORNL Irradiated Fuels Examination Laboratory staff.

1. INTRODUCTION AND BACKGROUND

Post-irradiation examination and elevated-temperature safety testing are being performed on compacts from the Advanced Gas Reactor (AGR) Fuel Development and Qualification Program's second irradiation experiment (AGR-2). The compacts in the AGR-2 irradiation experiment (Collin 2014) held either tristructural isotropic (TRISO)-coated particles containing uranium oxide fuel kernels (UO_2) or TRISO-coated particles containing fuel kernels with both uranium carbide and uranium oxide phases (UCO). In UO_2 TRISO particles, oxygen released by uranium fission can react with the surrounding carbon in the buffer layer to form carbon monoxide (CO). Excess CO can lead to various irradiation performance issues under certain operating conditions, such as pressure-induced fracture, kernel migration, and silicon carbide (SiC) corrosion (Petti et al. 2002, Minato et al. 1991). In UCO TRISO particles, CO formation is reduced because the chemical potential for oxidation of uranium carbide is lower than for oxidation of carbon (Homan et al. 1977).

The ORNL Core Conduction Cooldown Test Facility (CCCTF) was used to conduct isothermal safety tests of AGR-2 compacts by heating the compacts in helium to a target temperature and holding at this temperature for typically 300 h. Hunn et al. (2018a) reported summary results of 1,600 and 1,800°C safety tests on AGR-2 UCO compacts and 1,600 and 1,700°C safety tests on AGR-2 UO_2 compacts. Significant cesium releases were observed when safety testing AGR-2 UO_2 Compacts 3-3-2 and 3-4-2 at 1,600°C for 300 h and AGR-2 UO_2 Compact 3-4-1 at 1,700°C for 162 h. In all three tests, the cesium releases were primarily due to CO corrosion of the SiC layers in the UO_2 TRISO particles. The safety-tested UCO compacts did not exhibit CO corrosion, and the cumulative cesium release fractions at the end of the UCO compact safety tests were much lower than what were observed for the UO_2 compact safety tests.

This report presents the results from the 1,500°C safety test and post-safety-test destructive examination of AGR-2 UO_2 Compact 3-1-1. Table 1-1 shows the calculated average burnup in percent fissions per initial metal atom (FIMA), the average fast neutron fluence for neutron energies > 0.18 MeV, and the average compact temperatures during irradiation for all four safety-tested AGR-2 UO_2 compacts.

Table 1-1. Irradiation and safety test conditions for the AGR-2 UO_2 compacts

Compact ID [a]	Fabrication ID [b]	Safety test (°C)	Burnup [c] (% FIMA)	Fast fluence [c] (n/m^2)	Temperature [d] (°C)		
					TAVA	TA_{min}	TA_{max}
AGR-2 3-1-1	LEU11-OP2- Z029	1,500	10.60	3.41×10^{25}	1,011	900	1,083
AGR-2 3-3-2	LEU11-OP2- Z034	1,600	10.54	3.53×10^{25}	1,062	999	1,105
AGR-2 3-4-2	LEU11-OP2- Z150	1,600	10.69	3.50×10^{25}	1,013	904	1,085
AGR-2 3-4-1	LEU11-OP2- Z188	1,700	10.62	3.47×10^{25}	1,013	901	1,085

[a] The X-Y-Z compact identification (ID) numbering convention denotes the compact's location in the irradiation test train: *capsule-level-stack* (Collin 2014).

[b] Physical properties data for individual compacts are available and referenced by fabrication ID (Hunn, Montgomery, and Pappano 2010, 73–84).

[c] Burnup (Sterbentz 2014, Table 6) and fast fluence (Sterbentz 2014, Table 12) are based on physics calculations.

[d] Time-average, volume-average (TAVA) temperature; time-average minimum (TA_{min}) temperature; and time-average maximum (TA_{max}) temperature are based on thermal calculations (Hawkes 2014, Table 4).

2. SAFETY TEST RESULTS

The estimated time-dependent releases of typically tracked fission products during the 1,500°C safety test of Compact 3-1-1 are shown in Figure 2-1. Table 2-1 shows the cumulative releases of these isotopes as determined by the post-safety-test analyses of all the deposition cups, the CCCTF internal tantalum parts, and the graphite holder in which the compact resided throughout the test. Table 2-1 also shows the relative fractions of each measured isotope on each component group at the end of the safety test. To generate the estimated time-dependent compact releases plotted in Figure 2-1, the deposition cup collection efficiency for each isotope was assumed to be constant and equal to the relative fraction of each isotope deposited on the cups. Details of the CCCTF design and the process used to analyze the fission product release data were reported previously (Baldwin et al. 2012). As expected, collection efficiencies for silver and cesium were high because these elements are volatile at 1,500°C. The measured fraction of ^{137}Cs that was collected on the cups appears to be lower than ^{134}Cs, but this is an artifact of hot cell contamination that dominated the measured values for ^{137}Cs on the tantalum parts and graphite holder; therefore, the collection efficieny for ^{134}Cs was used for both cesium isotopes. The collection efficiencies for strontium and europium were low, which is typical when releases are low and is due to a holdup of these elements in the graphite holder. Because of this holdup, the estimated time-dependent releases that were calculated for ^{90}Sr and ^{154}Eu are highly uncertain.

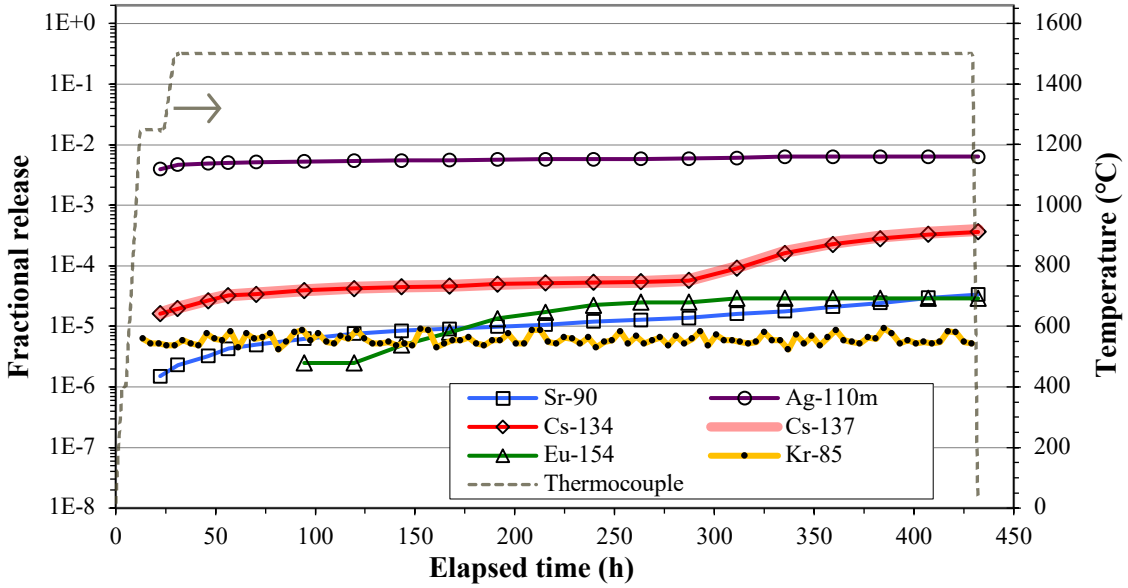

Figure 2-1. Release of fission products from Compact 3-1-1 during the 1,500°C safety test.

Table 2-1. Fission product distribution on furnace internal components after the Compact 3-1-1 safety test

Component	^{90}Sr	^{110m}Ag	^{134}Cs	^{137}Cs	^{154}Eu	^{155}Eu
Deposition cups [a]	12.4%	~100%	98.3%	89.6%	6.5%	1.3%
Tantalum parts	18.7%	~0%	1.3%	9.1%	~0%	~0%
Graphite holder	68.9%	~0%	0.4%	1.3%	93.5%	98.7%
Cumulative release [b]	3.35E-5 (0.052)	6.37E-3 (9.83)	3.62E-4 (0.56)	3.90E-4 (0.60)	2.90E-5 (0.045)	6.78E-6 (0.010)

[a]Values are the cumulative fractions collected on all deposition cups.
[b]Values are the released fractions of the calculated compact inventories and the equivalent fractions of the average inventories per particle (in parentheses).

2.1 CESIUM RELEASE DURING SAFETY TESTING

The amount of cesium released during the Compact 3-1-1 safety test indicated the presence of at least one particle with a SiC layer that failed to exhibit normal fission product retention during the safety test. Figure 2-2 highlights the cesium fractional release, and Figure 2-3 shows the same data in terms of the release rate. The cesium release rate rose significantly during the 24 h period when Cup 15 was in the furnace. Cup 15 was inserted 287 h after the start of the test (after 256 h at 1,500°C). The original plan was to terminate the safety test after 300 h of exposure at 1,500°C, which is the standard AGR safety test period. However, because the increased cesium activity on Cup 15 indicated SiC failure, the test was extended by an additional 100 h to allow further observation. The cesium release rate peaked during the Cup 16 residence period (280–304 h at 1,500°C), and then the rate consistently decreased until the test was terminated. The cesium release rate reduction after 304 h at 1,500°C indicated that the failed SiC particle or particles had released the majority of their unretained cesium and that no additional SiC failure occurred in other particles. The total fractional ^{134}Cs release of 6.37E-3, which corresponds to 56% of the inventory in an average particle, indicates that the SiC failure was most likely limited to a single particle; this is supported by the deconsolidation leach-burn-leach (DLBL) results discussed in Section 3.

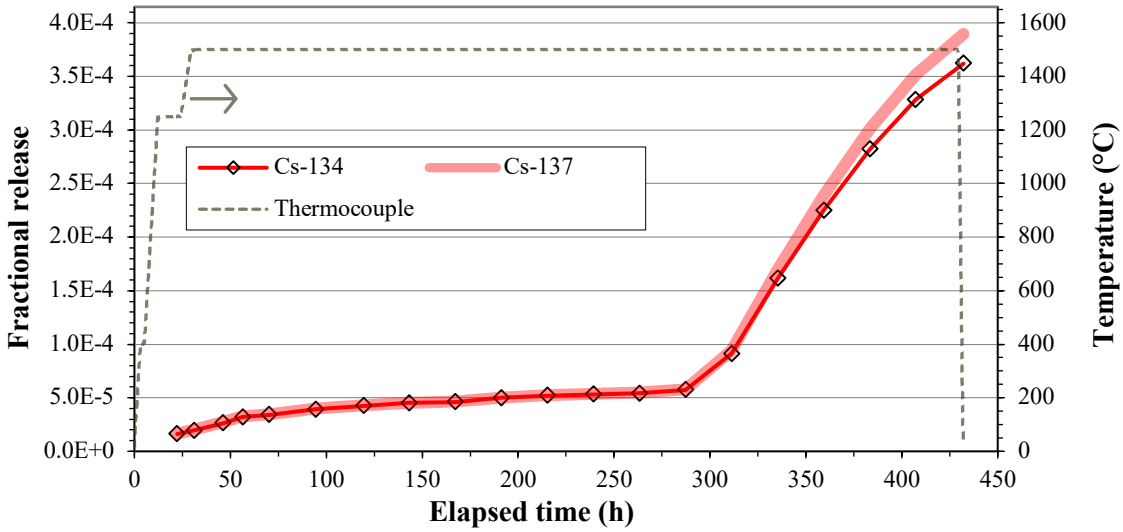

Figure 2-2. Fractional release of cesium from Compact 3-1-1 during the 1,500°C safety test.

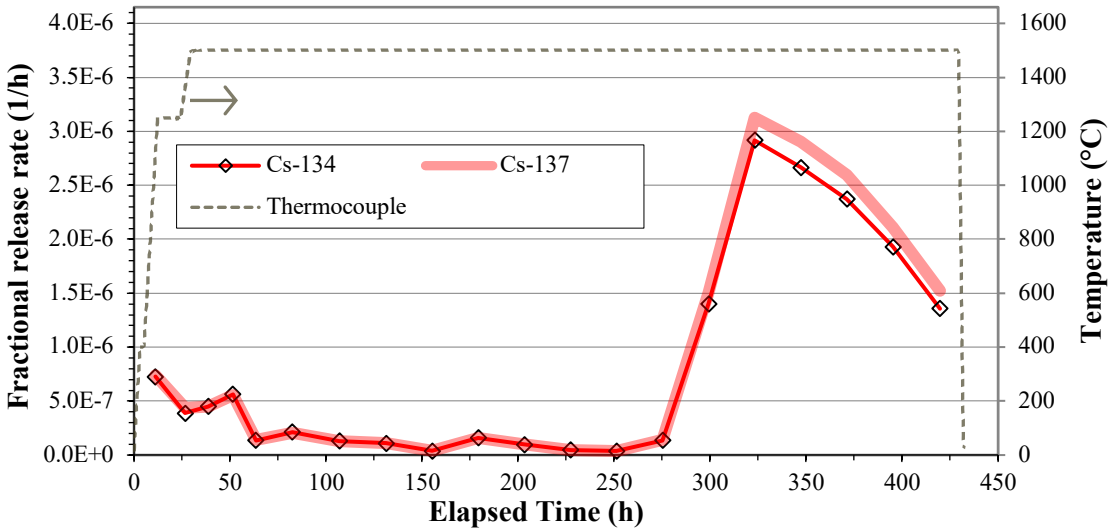

Figure 2-3. Cesium release rate from Compact 3-1-1 during the 1,500°C safety test.

The four deposition cups that were in the furnace during the first 56.5 h of the test showed a higher cesium release rate than the ten cups that were in the furnace during the next 230.8 h. Cup 1 was in the furnace while it was heating from room temperature to 1,250°C, and Cup 2 was in the furnace while it was heating from 1,250°C to 1,500°C. Cup 3 and Cup 4 were resident during the first 25.5 h at 1,500°C. The cumulative ^{134}Cs release during the initial 56.5 h was 0.05 particle equivalents. The cumulative ^{134}Cs release during the next 230.8 h was 0.04 particle equivalents. The slightly elevated cesium release rate at the beginning of the test was not an unusual behavior, and the cesium collected on the cups during this period could have been cesium that was initially residing in the compact matrix and/or cesium that was present as contamination in the CCCTF. However, 0.05 particle equivalents is higher than what is typically observed at the start of a safety test in the absence of particle failure. The cumulative cesium releases during this same timeframe at the start of the 1,600°C safety tests of Compact 3-3-2 and Compact 3-4-2 were less than 0.01 particle equivalents (Hunn et al. 2015). Before the cesium release rate spiked during the Cup 15 residence period, the cumulative fractional cesium releases from Compact 3-1-1 were 5.75E-5 for ^{134}Cs and 5.81E-5 for ^{137}Cs. This equates to 9% of the average inventory in one particle. A release of 0.09 particle equivalents is also high compared with typical safety tests of compacts without failed SiC in which the cesium release is usually below 0.02 particle equivalents (Hunn et al. 2018a).

There are several possible explanations for the atypically high amount of cesium detected in the CCCTF during the 1,500°C safety test of Compact 3-1-1 before the obvious indication of SiC failure provided by the significant increase in the cesium release rate after 256 h at 1,500°C. First, an unusually high amount of cesium could have been in the compact matrix due to unusually high uranium contamination during fabrication or an unexpected release of cesium during irradiation. However, this scenario cannot explain the higher than normal amount of cesium observed after the first 56.5 h of the test because most of the cesium in the matrix should have been released from the compact during the initial 56.5 h period. Second, some cesium could have been transferred to the cups from cesium-contaminated CCCTF furnace components. Cesium contamination in the CCCTF furnace was the dominant source of cesium collected on most of the deposition cups during the AGR-2 UCO Compact 6-4-2 and AGR-2 UCO Compact 6-4-3 safety tests (Hunn et al. 2019a). This contamination was primarily due to very high cesium releases during 1,700°C safety tests of AGR-2 UO_2 compacts, and its contribution during the UCO safety tests was differentiated from cesium released from the UCO compacts by the measured ^{134}Cs/^{137}Cs ratio, which was roughly twice as high for the lower enriched UO_2 fuel. It was determined that the contamination was mainly located on the shutters that serve as heat shields for the airlock gate valve when a deposition cup is removed from the CCCTF, and replacement of the airlock assembly is planned before AGR-5/6/7 safety testing. Prior to the Compact 3-1-1 safety test, the airlock heat shields were gently wiped with a damp rag to try to remove the cesium contamination, but the effectiveness of this cleaning is unknown. It cannot be determined whether the cesium collected during the Compact 3-1-1 safety test included a contribution from any residual contamination remaining in the airlock assembly because the ^{134}Cs/^{137}Cs ratio for Compact 3-1-1 was not significantly different from the AGR-2 UO_2 compacts tested at 1,700°C. Third, the atypically high amount of cesium detected during the Compact 3-1-1 safety test before the cesium release rate spiked could be related to a gradual reduction in the retention capability of the SiC layer in the particle that eventually released cesium at a higher rate during the Cup 15 residence period. This third explanation appears to be supported by the observed silver release discussed in Section 2.3.

2.2 KRYPTON RELEASE DURING SAFETY TESTING

By the time the CCCTF furnace reached 1,500°C, the ^{85}Kr activity in the sweep gas trap was ~1.5% of one particle equivalent, and this activity did not increase measurably throughout the remainder of the test. The source of this early ^{85}Kr release could have been ^{85}Kr sequestered in the compact matrix and/or outer pyrolytic carbon (OPyC) layers. There was not enough ^{85}Kr release to indicate the presence of a particle with failed TRISO. In addition, the lack of any increase in ^{85}Kr release in conjunction with the large spike in the cesium release rate indicates that the particle with failed SiC had at least one intact, gas-tight pyrolytic carbon layer, probably the OPyC layer based on other observations of particles with failed SiC (Hunn et al. 2014).

2.3 SILVER RELEASE DURING SAFETY TESTING

Figure 2-4 highlights the fractional release of ^{110m}Ag, and Figure 2-5 shows the same data in terms of the fractional release rate. The initial silver release from Compact 3-1-1 is consistent with observations of ^{110m}Ag release during the initial heating at the beginning of previous AGR safety tests. This silver is understood to come from silver that is released through intact SiC during irradiation and temporarily sequestered in the matrix and/or OPyC until a compact is heated above the irradiation temperature during safety testing. However, this initial release is typically followed by a negligible additional release once the sequestered silver is flushed out (Morris 2014) unless additional release is driven by particle failure or thermal diffusion, which is usually only evident at 1,800°C for the relatively short 300 h safety test period. Figure 2-4 and Figure 2-5 show that, although the ^{110m}Ag release rate dropped after the compact reached 1,500°C, there was still a measurable and relatively significant ^{110m}Ag accumulation after the initial release. There was also a spike in the ^{110m}Ag release rate that corresponded with the spike in the cesium release rate. About one particle equivalent of ^{110m}Ag was released during the second half of the safety test, which encompassed the observed SiC failure event. The overall silver release behavior agrees well with the observed cesium release behavior. This agreement supports the hypothesis that the minor silver and cesium releases observed prior to the spike in their release rates could have been related to gradual reduction in the retention capability of the SiC layer in the particle that eventually experienced gross SiC failure during the Cup 15 residence period.

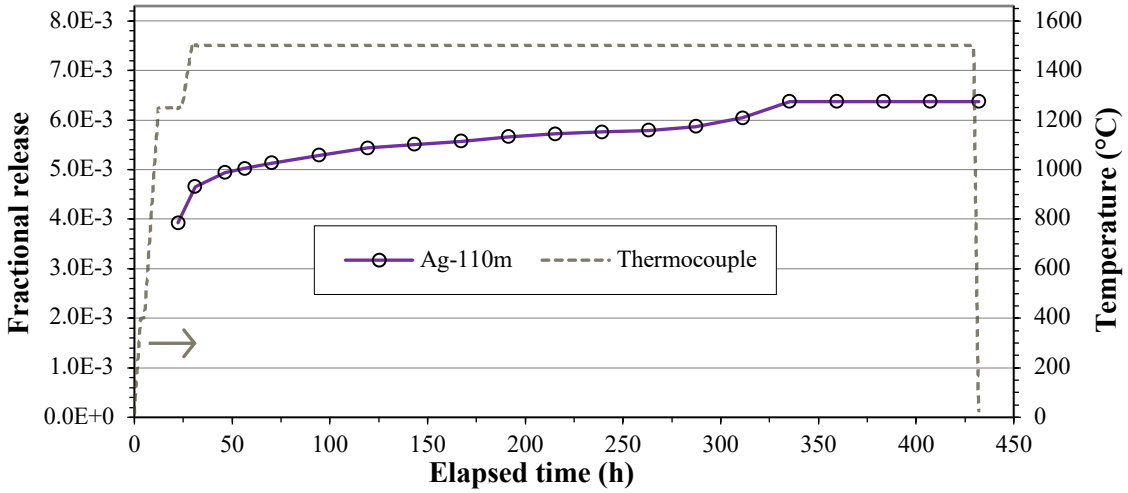

Figure 2-4. Fractional release of silver from Compact 3-1-1 during the 1,500°C safety test.

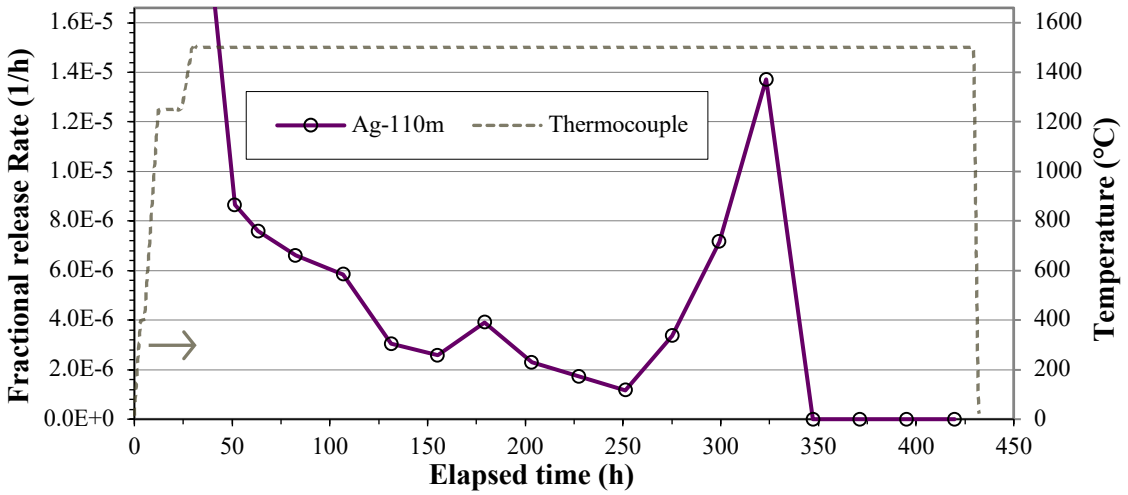

Figure 2-5. Silver release rate from Compact 3-1-1 during the 1,500°C safety test.

2.4 STRONTIUM AND EUROPIUM RELEASE DURING SAFETY TESTING

The total strontium and europium releases were low, and there were no measurable time dependences. As discussed at the beginning of Section 2, the holdup of these elements in the graphite precludes acquiring time-dependent information when the total releases are low. In addition, holdup in the matrix and OPyC delays release of strontium and europium from the compact once it is released from a particle. Therefore, any time-dependent behavior related to an elevated release from the particle with failed SiC could not be observed. The cumulative release fraction of ^{90}Sr was 3.35E-5 or ~0.05 particle equivalents (Table 2-1). The values for ^{154}Eu were similar at 2.90E-5 or ~0.04 particle equivalents. The cumulative release data for ^{155}Eu are less reliable, and ^{155}Eu release was not plotted in Figure 2-1 because the lower energy gamma emission from ^{155}Eu could only be measured on Cup 13.

3. DECONSOLIDATION AND LEACH-BURN-LEACH ANALYSIS

Compact 3-1-1 was deconsolidated and subjected to the standard DLBL procedure described by Hunn et al. (2013) and Hunn and Montgomery (2020) to recover the TRISO particles for survey with the ORNL Irradiated Microsphere Gamma Analyzer (IMGA) and to measure the amount of exposed actinides and fission products remaining in the compact. Table 3-1 shows data for several uranium and plutonium isotopes that were detected in the acid solutions. The amounts of uranium and plutonium collected in the deconsolidation acid and first preburn leach of the particles and matrix debris were <1%. This indicates that no kernels were exposed, confirming the conclusion based on the low observed ^{85}Kr release that stated there were no failed TRISO particles during safety testing. The uranium content increased slightly in the second preburn leach, and the first postburn leach of the matrix debris detected around one particle equivalent of exposed uranium and plutonium. This indicates that a particle was broken, probably at the end of the second preburn leach when the particles and matrix debris in the Soxhlet thimble were rinsed to collect residual acid after removing the thimble from the Soxhlet extraction apparatus. After the second preburn leach, the rinsed particles and matrix debris were boiled in acid to further digest the matrix and remove residual matrix from the surface of the TRISO particles before sieving to separate the particles from the digestion acid and matrix debris. It is presumed that the exposed kernel was dissolved during the digestion, so that most of what was in the kernel was washed through the sieve with the matrix debris. After boiling off most of the acid, the matrix was dried, burned, and the postburn matrix ash was leached twice. Any kernel material in the matrix debris would be dissolved in the first postburn matrix leach. Table 3-2 shows the analysis results for various radioactive isotopes, and Table 3-3 show the analysis results for various stable isotopes. The data for many of these isotopes exhibit similar evidence for the presence of one exposed kernel at the end of the second preburn leach, with most of the kernel content appearing in the first postburn matrix leach. There were no indications of additional kernel exposures due to particle breakage during the last three leaches.

Table 3-1. Exposed U and Pu detected by DLBL

DLBL step	^{235}U	^{236}U	^{238}U	^{239}Pu	^{240}Pu
Deconsolidation acid	3.35E-6 (0.0052)	1.46E-6 (0.0023)	3.75E-6 (0.0058)	2.87E-6 (0.0044)	3.52E-6 (0.0054)
Preburn leach 1	9.12E-7 (0.0014)	5.52E-7 (0.0009)	1.17E-6 (0.0018)	9.40E-7 (0.0015)	9.57E-7 (0.0015)
Preburn leach 2	5.51E-6 (0.0085)	5.04E-6 (0.0078)	6.72E-6 (0.010)	3.67E-6 (0.0057)	3.95E-6 (0.0061)
Postburn matrix leach 1	9.12E-4 (1.407)	7.69E-4 (1.186)	6.85E-4 (1.058)	5.87E-4 (0.906)	6.49E-4 (1.001)
Postburn matrix leach 2	7.96E-6 (0.012)	6.65E-6 (0.010)	6.68E-6 (0.010)	6.30E-6 (0.0097)	6.80E-6 (0.010)
Postburn particle leach 1 [a]	2.59E-5 (0.040)	9.27E-6 (0.014)	1.49E-5 (0.023)	9.33E-6 (0.014)	1.12E-5 (0.017)
Postburn particle leach 2 [a]	3.43E-6 (0.0053)	1.52E-6 (0.0023)	4.62E-6 (0.0071)	1.65E-6 (0.0026)	2.18E-6 (0.0034)
Total	9.59E-4 (1.479)	7.93E-4 (1.224)	7.23E-4 (1.116)	6.12E-4 (0.944)	6.77E-4 (1.045)

Note: Values are reported as compact inventory fractions and particle equivalents (in parentheses).
Note: Values that primarily contributed to the total for each isotope are highlighted.
[a]A scaling factor was applied to account for ~207 out of the ~1,543 particles not included in the analysis.

Table 3-2. Exposed compact inventory fractions of typically tracked beta/gamma-emitting fission products detected by DLBL

DLBL step	^{90}Sr [a]	^{106}Ru	^{110m}Ag	^{125}Sb	^{134}Cs	^{137}Cs	^{144}Ce	^{154}Eu	^{155}Eu
Deconsolidation acid	4.73E-5 (0.073)	<1.57E-6 (<0.0024)	<2.27E-4 (<0.35)	<2.95E-6 (<0.0046)	2.25E-6 (0.0035)	4.43E-6 (0.0068)	<1.12E-6 (<0.0017)	2.22E-5 (0.034)	2.67E-5 (0.041)
Preburn leach 1	1.95E-4 (0.301)	<2.99E-6 (<0.0046)	<3.95E-4 (<0.61)	<5.97E-6 (<0.0092)	5.51E-6 (0.0085)	1.39E-5 (0.021)	<2.19E-6 (<0.0034)	6.23E-5 (0.096)	7.53E-5 (0.012)
Preburn leach 2	1.27E-5 (0.020)	<6.21E-6 (<0.0096)	<5.13E-4 (<0.79)	<1.41E-5 (<0.022)	7.78E-6 (0.012)	3.20E-5 (0.049)	<3.99E-6 (<0.0062)	1.39E-5 (0.022)	1.97E-5 (0.030)
Postburn matrix leach 1	4.49E-4 (0.693)	3.04E-5 (0.047)	<1.05E-3 (<1.62)	4.42E-5 (0.068)	1.05E-4 (0.162)	1.60E-4 (0.247)	7.41E-4 (1.144)	4.65E-4 (0.718)	5.80E-4 (0.896)
Postburn matrix leach 2	4.71E-6 (0.0073)	3.55E-6 (0.0055)	<2.69E-4 (<0.42)	1.31E-5 (0.020)	4.36E-6 (0.0067)	7.48E-6 (0.012)	6.59E-6 (0.010)	8.46E-6 (0.013)	7.40E-6 (0.011)
Postburn particle leach 1 [b]	4.95E-5 (0.076)	<5.63E-6 (<0.0087)	<8.53E-4 (<1.32)	<8.54E-6 (<0.013)	1.90E-5 (0.029)	2.89E-5 (0.045)	9.91E-6 (0.015)	4.06E-5 (0.063)	5.37E-5 (0.083)
Postburn particle leach 2 [b]	1.97E-6 (0.0030)	4.14E-6 (0.0064)	<6.53E-4 (<1.01)	<5.82E-6 (<0.0090)	3.48E-6 (0.0054)	5.73E-6 (0.0088)	<2.51E-6 (<0.0039)	<2.43E-6 (<0.0037)	<2.49E-6 (<0.0038)
Total	7.60E-4 (1.173)	3.81E-5 (0.059)	- -	5.73E-5 (0.088)	1.48E-4 (0.228)	2.53E-4 (0.390)	7.58E-4 (1.169)	6.13E-4 (0.946)	7.63E-4 (1.178)

Note: Values are reported as compact inventory fractions and particle equivalents (in parentheses).
Note: Values that primarily contributed to the total for each isotope are highlighted.
Note: A less-than value indicates that the concentration in the leachate was below the minimum detectable limit; these values are not included in the totals.
[a]Chemical separation and beta analysis were used to measure ^{90}Sr; other isotopes were measured by gamma spectrometry.
[b]A scaling factor was applied to account for ~207 out of the ~1,543 particles not included in the analysis.

Table 3-3. Exposed compact inventory fractions of stable isotopes of interest detected by DLBL

DLBL step	^{105}Pd	^{109}Ag	^{133}Cs	^{139}La	^{140}Ce	^{141}Pr	^{146}Nd	^{152}Sm	^{153}Eu	^{156}Gd
Deconsolidation acid	<1.85E-5 (<0.029)	1.30E-4 (0.200)	4.86E-6 (0.0075)	2.24E-5 (0.035)	1.55E-5 (0.024)	3.38E-6 (0.0052)	2.63E-6 (0.0041)	1.05E-5 (0.016)	4.19E-5 (0.065)	3.47E-5 (0.054)
Preburn leach 1	<2.08E-5 (<0.032)	1.61E-4 (0.249)	1.68E-5 (0.026)	8.21E-5 (0.127)	7.42E-5 (0.115)	7.93E-6 (0.012)	5.26E-6 (0.0081)	3.57E-5 (0.055)	1.26E-4 (0.194)	1.12E-4 (0.172)
Preburn leach 2	<2.83E-5 (<0.044)	1.08E-4 (0.167)	3.34E-5 (0.052)	1.76E-5 (0.027)	2.08E-5 (0.032)	5.36E-6 (0.0083)	4.43E-6 (0.0068)	<1.18E-5 (<0.018)	2.42E-5 (0.037)	3.09E-5 (0.048)
Postburn matrix leach 1	1.51E-4 (0.233)	1.87E-4 (0.289)	1.38E-4 (0.212)	9.06E-4 (1.397)	8.62E-4 (1.331)	6.45E-4 (0.996)	5.52E-4 (0.851)	6.42E-4 (0.991)	5.92E-4 (0.914)	1.04E-3 (1.608)
Postburn matrix leach 2	<2.15E-5 (<0.033)	<1.88E-5 (<0.029)	4.89E-6 (0.0075)	1.10E-5 (0.017)	1.90E-5 (0.029)	6.24E-6 (0.0096)	5.39E-6 (0.0083)	<8.98E-6 (<0.014)	<1.18E-5 (<0.018)	<1.58E-5 (<0.024)
Postburn particle leach 1 [a]	3.06E-5 (0.047)	7.34E-5 (0.113)	2.99E-5 (0.046)	1.34E-4 (0.207)	9.88E-5 (0.152)	2.35E-5 (0.036)	1.88E-5 (0.029)	2.16E-5 (0.033)	8.89E-5 (0.139)	2.87E-4 (0.443)
Postburn particle leach 2 [a]	<3.53E-5 (<0.054)	9.59E-5 (0.148)	6.90E-6 (0.011)	5.22E-6 (0.0081)	6.83E-6 (0.011)	2.66E-6 (0.0041)	2.56E-6 (0.0039)	<1.48E-5 (<0.023)	<1.94E-5 (<0.030)	<2.59E-5 (<0.040)
Total	1.81E-4 (0.280)	7.56E-4 (1.167)	2.34E-4 (0.361)	1.18E-3 (1.818)	1.10E-3 (1.694)	6.94E-4 (1.071)	5.91E-4 (0.911)	7.10E-4 (1.096)	8.74E-4 (1.349)	1.51E-3 (2.324)

Note: Values are reported as compact inventory fractions and particle equivalents (in parentheses).
Note: Values that primarily contributed to the total for each isotope are highlighted.
Note: A less-than value indicates that the concentration in the leachate was below the minimum detectable limit; these values are not included in the totals.
[a]A scaling factor was applied to account for ~207 out of the ~1,543 particles not included in the analysis.

4. IMGA SURVEY OF DECONSOLIDATED TRISO PARTICLES

An IMGA survey of all the available particles was performed to find any particles with low cesium or cerium inventory. There were 1,517 TRISO particles separated from the matrix debris that were run through the IMGA and an estimated 25 additional particles that were trapped in small undigested chunks that could not be gamma counted for individual inventory. Of the 1,517 TRISO particles loaded into the IMGA, 1,509 particles were counted and 8 particles were dropped during the IMGA automated vacuum needle transfer that were unrecoverable. Figure 4-1 shows a histogram of the measured ^{137}Cs activity in each counted particle, $A_i(^{137}Cs)$, divided by its particle-specific calculated activity, which was based on an adjustment to the average calculated activity, $A_{calc}(^{137}Cs)$, using the normalized ^{106}Ru activity, $A_i(^{106}Ru)$, to account for variation in initial fissile inventory and burnup. Typically, this adjustment is done using the normalized ^{144}Ce activity (Hunn et al. 2013), but because the gamma emission rate was low after ~7.6 ^{144}Ce half-lives had passed, the longer lived ^{106}Ru activity was used (Hunn et al. 2019b). No abnormally low cesium particles were detected with IMGA. This is consistent with the conclusion that the one particle that was broken and leached during DLBL analysis was most likely the particle responsible for the cesium release during safety testing. Presumably, this particle had a failed SiC layer and an intact OPyC layer at the conclusion of the safety test, and the OPyC broke at the end of the second preburn leach, as discussed in Section 3.

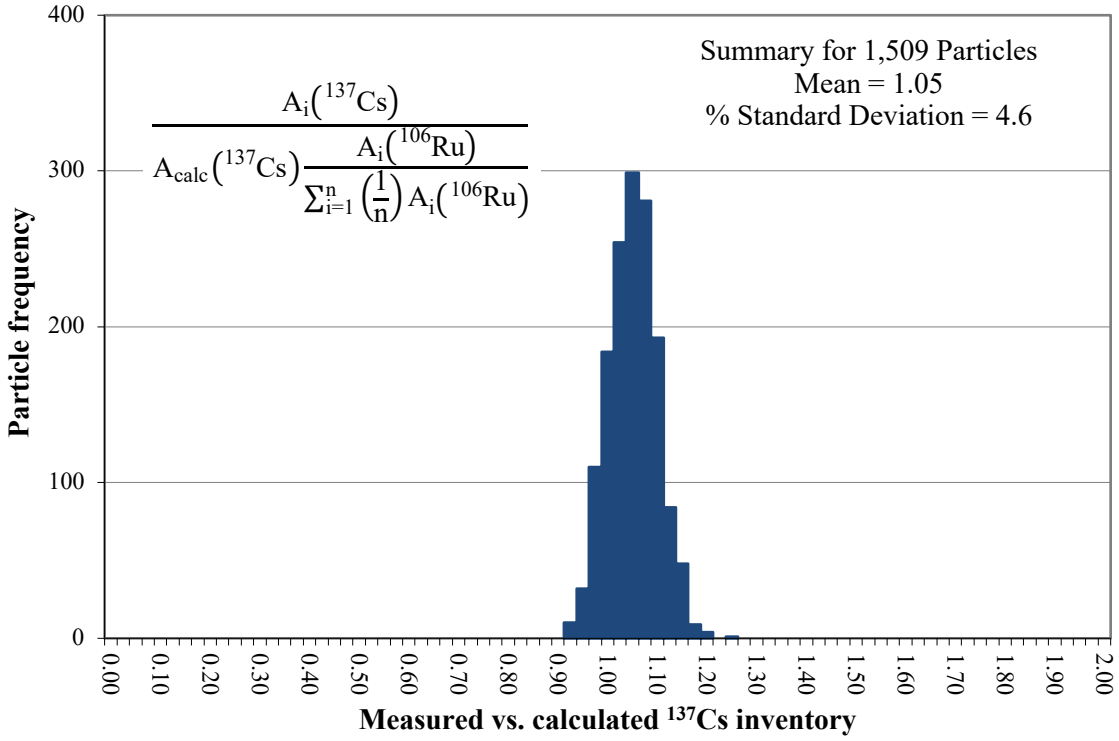

Figure 4-1. Ratio of the ^{137}Cs retained in 1,509 Compact 3-1-1 particles after the 1,500°C safety test vs. the calculated inventory adjusted using the measured ^{106}Ru for variation in fissionable material and burnup.

5. CONCLUSION

Compact 3-1-1 was safety tested by heating in helium to 1,500°C and holding it at temperature for ~400 h, in which the planned 300 h test was extended by 100 h because of an uptick in the cesium release rate after 256 h at 1,500°C. The cesium release rate peaked sometime between 280–304 h after the compact first reached a temperature of 1,500°C, then consistently decreased until the test terminated. The amount of cesium that was released during the safety test and the time dependence of the cesium release rate were consistent with the presence of one particle with failed SiC. The DLBL analysis performed after safety testing clearly indicated that one compromised particle was broken at the end of the second preburn leach and that the kernel material was dissolved. Based on the amount of cesium released during safety testing and the absence of any abnormally low cesium particles in the 1,509 particles counted with the IMGA, it is presumed that there was only one particle with failed SiC and that this particle was the particle that was leached during DLBL. The combined amount of cesium collected in the CCCTF and DLBL analyses was 0.79 particle equivalents of ^{134}Cs and 0.99 particle equivalents of ^{137}Cs. This amount of cesium is also consistent with the conclusion that only one particle experienced SiC failure during safety testing. The value for ^{137}Cs is slightly higher than the value for ^{134}Cs, which is probably due to the fact that the ^{137}Cs measurement is impacted more by hot cell contamination.

The amount of cesium released before 256 h at 1,500°C suggested that there was some cesium emitted from the particle with failed SiC before the obvious spike in the cesium release rate that indicated gross cesium retention failure. There was a spike in the ^{110m}Ag release rate that was concurrent with the spike in the cesium release rate, which indicated that the particle with failed SiC also released silver. Similar to what was observed for cesium, the time-dependent release of ^{110m}Ag suggested that there was some silver emitted from the particle with failed SiC before the obvious spike in the ^{110m}Ag release rate.

The amount of cesium released during the safety tests of the four AGR-2 UO_2 compacts listed in Table 1-1 increased exponentially with each 100°C increment. As discussed herein, the 1,500°C safety test of Compact 3-1-1 resulted in a ^{134}Cs release fraction of 3.6E-4. The two 300 h, 1,600°C safety tests resulted in ^{134}Cs release fractions of 2.1E-3 from Compact 3-3-2 and 9.3E-3 from Compact 3-4-2 (Hunn et al. 2015). The 1,700°C safety test of Compact 3-4-1 was terminated after 162 h because the radioactivity from the cesium release was approaching approved CCCTF operating limits. Although it was only heated at 1,700°C for 162 h, the ^{134}Cs release fraction from Compact 3-4-1 was 8.7E-2 (Hunn et al. 2018b). The Compact 3-1-1 particle with failed SiC was not recovered for microstructural analysis, so it cannot be concluded that CO corrosion was the cause of the SiC failure during the 1,500°C safety test. However, numerous particles were recovered from the other safety tested AGR-2 UO_2 compacts, and many of these showed strong evidence of CO corrosion (Morris et al. 2016). No CO corrosion was observed in particles from the safety-tested UCO compacts, and SiC failure fractions were much lower for the safety-tested UCO compacts compared with the safety-tested UO_2 compacts (Hunn et al. 2018a). This difference in behavior was due to the presence of the uranium carbide in the UCO kernels, which reduced the amount of CO that was formed during irradiation.

6. REFERENCES

Baldwin, Charles A., John D. Hunn, Robert N. Morris, Fred C. Montgomery, Chinthaka M. Silva, and Paul A. Demkowicz. 2012. "First Elevated Temperature Performance Testing of Coated Particle Fuel Compacts from the AGR-1 Irradiation Experiment." Paper HTR2012-3-027, *Proc. 6th International Topical Meeting on High Temperature Reactor Technology (HTR-2012)*. Tokyo, Japan, October 28–November 1, 2012. Also published in *Nucl. Eng. Des.* 271 (2014): 131–141.

Collin, Blaise P. 2014. *AGR-2 Irradiation Test Final As-Run Report.* INL/EXT-14-32277, Revision 2. Idaho Falls: Idaho National Laboratory.

Hawkes, Grant L. 2014. *AGR-2 Daily As-Run Thermal Analyses.* INL/ECAR-2476, Revision 1. Idaho Falls: Idaho National Laboratory.

Homan, Franklin J., Terrence B. Lindemer, Ernest L. Long, Jr., Terry N. Tiegs, and Ronald L. Beatty. 1977. "Stoichiometric Effects on Performance of High-Temperature Gas-Cooled Reactor Fuels from the U-C-O System." *Nucl. Tech.* 35:428–441.

Hunn, John D., Fred C. Montgomery, and Peter J. Pappano. 2010. *Data Compilation for AGR-2 UO_2 Compact Lot LEU11-OP2-Z.* ORNL/TM-2010/055, Revision 1. Oak Ridge: Oak Ridge National Laboratory.

Hunn, John D., Robert N. Morris, Charles A. Baldwin, Fred C. Montgomery, Chinthaka M. Silva, and Tyler J. Gerczak. 2013. *AGR-1 Irradiated Compact 4-4-2 PIE Report: Evaluation of As-Irradiated Fuel Performance with Leach Burn Leach, IMGA, Materialography, and X-ray Tomography*. ORNL/TM-2013/236, Revision 0. Oak Ridge: Oak Ridge National Laboratory.

Hunn, John D., Charles A. Baldwin, Tyler J. Gerczak, Fred C. Montgomery, Robert N. Morris, Chinthaka M. Silva, Paul A. Demkowicz, Jason M. Harp, Scott A. Ploger, Isabella J. van Rooyen, and Karen E. Wright. 2014. "Detection and Analysis of Particles with Failed SiC in AGR-1 Fuel Compacts." Paper HTR2014-31254, *Proc. 7th International Topical Meeting on High Temperature Reactor Technology (HTR-2014)*. Weihai, China, October 27–31, 2014. Also published in *Nucl. Eng. Des.* 360 (2016): 36–46.

Hunn, John D., Robert N. Morris, Charles A. Baldwin, and Fred C. Montgomery. 2015. *Safety-Testing of AGR-2 UO_2 Compacts 3-3-2 and 3-4-2*. ORNL/TM-2015/388, Revision 0. Oak Ridge: Oak Ridge National Laboratory.

Hunn, John D., Robert N. Morris, Fred C. Montgomery, Tyler J. Gerczak, Darren J. Skitt, Charles A. Baldwin, John A. Dyer, Grant W. Helmreich, Brian D. Eckhart, Zachary M. Burns, Paul A. Demkowicz, and John D. Stempien. 2018a. "Post-Irradiation Examination and Safety Testing of US AGR-2 Irradiation Test Compacts." Paper HTR2018-0010, *Proc. 9th International Topical Meeting on High Temperature Reactor Technology (HTR-2018)*. Warsaw, Poland, October 8–10, 2018.

Hunn, John D., Robert N. Morris, Fred C. Montgomery, Tyler J. Gerczak, Darren J. Skitt, Grant W. Helmreich, Brian D. Eckhart, and Zachary M. Burns. 2018b. *Safety-Testing and Post-Safety-Test Examination of AGR-2 UCO Compact 2-3-2 and AGR-2 UO_2 Compact 3-4-1*. ORNL/TM-2018/956, Revision 0. Oak Ridge: Oak Ridge National Laboratory.

Hunn, John D., Tyler J. Gerczak, Robert N. Morris, Fred C. Montgomery, Darren J. Skitt, Brian D. Eckhart, Zachary M. Burns. 2019a. *Safety-Testing and Destructive Examination of AGR-2 UCO Compact 6-4-3*. ORNL/TM-2019/1200, Revision 0. Oak Ridge: Oak Ridge National Laboratory.

Hunn, John D., Tyler J. Gerczak, Robert N. Morris, Fred C. Montgomery, Darren J. Skitt, Brian D. Eckhart, Zachary M. Burns. 2019b. *Safety-Testing and Destructive Examination of AGR-2 UCO Compact 2-1-2*. ORNL/TM-2019/1201, Revision 0. Oak Ridge: Oak Ridge National Laboratory.

Hunn, John D., and Fred C. Montgomery. 2020. *Data Acquisition Method: Leach-Burn-Leach Analysis of Irradiated Fuel Compacts Using a Soxhlet Extractor in the 3525 Hot Cell*. AGR-CHAR-DAM-37, Revision 4. Oak Ridge: Oak Ridge National Laboratory.

Minato, Kazuo, Toru Ogawa, Satoru Kashimura, Kousaku Fukuda, Ishio Takahashi, Michio Shimizu, and Yoshinobu Tayama. 1991. "Carbon Monoxide-Silicon Carbide Interaction in HTGR Fuel Particles," *J. Mater. Sci.* 26: 2379–2388.

Morris, Robert N., Paul A. Demkowicz, John D. Hunn, Charles A. Baldwin, and Edward L. Reber. 2014. "Performance of AGR-1 High Temperature Reactor Fuel During Post-Irradiation Heating Tests." Paper HTR2014-31135, *Proc. 7th International Topical Meeting on High Temperature Reactor Technology (HTR-2014)*. Weihai, China, October 27–31, 2014. Also published in *Nucl. Eng. Des.* 306 (2016): 24–35.

Morris, Robert N., John D. Hunn, Charles A. Baldwin, Fred C. Montgomery, Tyler J. Gerczak, and Paul A. Demkowicz. 2016. "Initial Results from Safety Testing of US AGR-2 Irradiation Test Fuel." Paper HTR2016-18574, *Proc. 8th International Topical Meeting on High Temperature Reactor Technology (HTR-2016)*. Las Vegas, Nevada, November 6–10, 2016. Also published in *Nucl. Eng. Design* 329 (2018): 124–133.

Petti, David A., John T. Maki, Jacopo Buongiorno, Richard R. Hobbins, and Gregory K. Miller. 2002. *Key Differences in the Fabrication, Irradiation and Safety Testing of U.S. and German TRISO-coated Particle Fuel and Their Implications on Fuel Performance*. INEEL/EXT-02-00300, Revision 0. Idaho Falls: Idaho National Laboratory.

Sterbentz, James W. 2014. *JMOCUP As-Run Daily Depletion Calculation for the AGR-2 Experiment in the ATR B-12 Position.* ECAR-2066, Revision 2. Idaho Falls: Idaho National Laboratory.